Emission of Spin-Correlated Matter-Wave Jets from Spinor Bose-Einstein Condensates

Emission of Spin-Correlated Matter-Wave Jets from Spinor Bose-Einstein Condensates

Kyungtae Kim,[1] Junhyeok Hur,[1] SeungJung Huh,[1] Soonwon Choi,[2,3] and Jae-yoon Choi[1,*]
[1]*Department of Physics, Korea Advanced Institute of Science and Technology, Daejeon 34141, Korea*
[2]*Department of Physics, University of California Berkeley, Berkeley, California 94720, USA*
[3]*Center for Theoretical Physics, Massachusetts Institute of Technology, Cambridge, Massachusetts 02139, USA*

(Received 8 February 2021; accepted 16 June 2021; published 22 July 2021)

We report the observation of matter-wave jet emission in a strongly ferromagnetic spinor Bose-Einstein condensate of ^{7}Li atoms. Directional atomic beams with $|F=1, m_F=1\rangle$ and $|F=1, m_F=-1\rangle$ spin states are generated from $|F=1, m_F=0\rangle$ state condensates or vice versa. This results from collective spin-mixing scattering events, where spontaneously produced pairs of atoms with opposite momentum facilitates additional spin-mixing collisions as they pass through the condensates. The matter-wave jets of different spin states ($|F=1, m_F=\pm1\rangle$) can be a macroscopic Einstein-Podolsky-Rosen state with spacelike separation. Its spin-momentum correlations are studied by using the angular correlation function for each spin state. Rotating the spin axis, the inter- and intraspin-momentum correlation peaks display a high-contrast oscillation, indicating collective coherence of the atomic ensembles. We provide numerical calculations that describe the experimental results at a quantitative level. Our Letter paves the way to generating macroscopic quantum entanglement with the spin and motional degree of freedom with massive particles. It has a wide range of applications from quantum information science to the fundamental studies of quantum entanglement.

DOI: 10.1103/PhysRevLett.127.043401

The collective scattering processes in many-body systems can lead to remarkable counterintuitive phenomena, due to quantum interference effects. Superradiance in an atomic ensemble is a prominent example, where the spontaneous emission process occurs cooperatively, emitting a directional light with an enhanced decay rate [1]. Superradiant scattering is observed in degenerate Bose [2] and Fermi gases [3] and is often described as a self-amplified atom-light scattering process [2,4,5]. Atoms scattered by incoming light can interfere with condensates at rest, forming a matter-wave grating that diffracts successive laser light, enhancing the amplitude of the density modulation. These collective behaviors are not solely restricted to the optical domain, but can also extend to matter waves, where directional atomic beams are generated without external light fields [6]. Under a periodic driving of scattering length, density modulations are spontaneously developed, stimulating further pairwise collision processes with a certain direction given by the density modulation [6,7]. This ends up as a directional atomic beam, resembling fireworks, contrasting a diffusive spherical shell structure out of uncorrelated *s*-wave collisions [8].

Recent studies of matter-wave emissions have offered new opportunities to study complex correlations in the high-harmonic generation process [9], quantum phenomena in a noninertial frame [10], and dissipative many-body quantum dynamics [11]. Such efforts can provide new directions for producing nonclassical quantum states of atomic spins. In spinor Bose-Einstein condensates (BECs), for example, correlated spin states like the squeezed vacuum state [12–14] have been generated via spin-mixing collisions, to explore fundamental questions of quantum physics [15,16] and its application to quantum metrology [17–20]. However, most of such experiments have focused on the low kinetic energy regime, where the created spin pairs are localized in the trapping potential with their source, challenging the local addressing and manipulation of the quantum state. One way to overcome this hurdle would be to realize directional superradiant collisions in a spin manifold, which could generate a macroscopic Einstein-Podolsky-Rosen (EPR) state of atoms [21–23].

In this Letter, we report the emission of spin-correlated matter-wave jets from spinor BECs of ^{7}Li atoms. The directional atomic beams of $|F=1, m_F=\pm1\rangle(|\uparrow\rangle, |\downarrow\rangle)$ spin states are generated from $|F=1, m_F=0\rangle$ state condensates or vice versa. The kinetic energy of the atomic beam is high enough to escape the trapping potential, where we take advantage of strongly ferromagnetic spin interaction to facilitate the matter-wave amplification of fast-moving particles. The matter waves with opposite spin states can be a macroscopic EPR state, and its spin-momentum correlation is revealed by angular correlation functions between emitted spin states. To investigate nonclassical correlations, we coherently rotate the spin states and study the responses of the correlation functions at various rotation angles. The momentum correlation peaks among these spin states exhibit a high-contrast oscillation as a function of the rotation angle, suggesting that the ensembles of atoms with opposite spins still maintain collective coherence to exhibit interference patterns.

Our experimental sequences start by preparing an $F = 1$ spinor condensate of ^{7}Li atoms in a quasi-two-dimensional (2D) optical trap [24]. The condensates are initially in a polar phase due to a few Gauss of the magnetic field along the z axis. To observe the matter-wave jets from spinor BECs, we apply a rf pulse to the trapped condensates, making equal population of $|\uparrow\rangle$ and $|\downarrow\rangle$ states. When the quadratic Zeeman energy $q = h \times 1-5$ kHz [Fig. 1(a)] dominates the spin-dependent interaction energy ($|c| = h \times 160$ Hz), the initial state is unstable, producing pairs of atom in the $|0\rangle$ state owing to the presence of quantum fluctuations [25]. The spontaneously created atom pairs obtain kinetic energy from the quadratic Zeeman energy and propagate in opposite direction due to momentum conservation [Fig. 1(b)]. The moving atoms can interfere with stationary condensates in the $|\uparrow\rangle$ and $|\downarrow\rangle$ states via spin-mixing Hamiltonian, displaying spatial modulations in the scattering amplitude that stimulates a further pair generation process [5,22]. This, in turn, leads to self-amplification of the modulation amplitude and the emission of a directional atomic beam in the horizontal plane constrained by strong 2D potential (see Supplemental Material [26]).

The spin-mixing collisional strength is characterized by the spin-dependent interaction coefficient (c_2). We note that the ^{7}Li atoms are favorable for observing the matter-wave jets because of their strong spin interactions [24]. The spin-dependent interaction coefficient of the atoms is as large as 46% of the spin-independent interaction coefficient. Therefore, the grating formed by spin-mixing interaction is weakly dephased more by the source condensates than the other alkali atoms [40], and the traveling spin pairs can be amplified self-consistently.

The emission of matter-wave jets in the $|0\rangle$ state is shown in Fig. 1(c). Stern-Gerlach spin separated absorption images are used to resolve the source condensates in the trap and the created pairs, so that we are able to study its dynamics under various hold times t_h after the rf pulse. In the first few milliseconds of hold time, the condensates are stable with no populations in the $|0\rangle$ state. Then, radially propagating atomic beams with narrow angular width, matter-wave jets, suddenly appear at $t_h \sim 5$ ms. After 10 ms of hold time, the matter-wave jets start to escape the BECs. The angular pattern of the jets is random in each experimental run, and the jets seem to have their own partner in the opposite direction. Moreover, we find that the kinetic energy per atom (E_k) of the matter-wave jets is almost equal to the quadratic Zeeman energy [26], indicating that the atom pairs are created from the source condensates after the spin-changing scattering process.

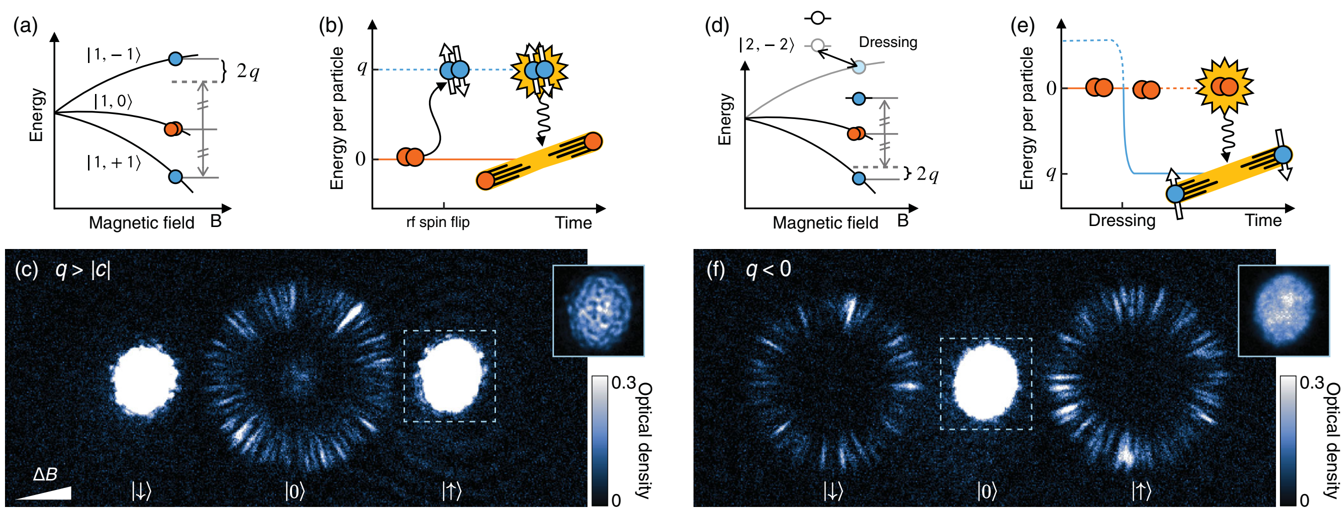

FIG. 1. Emission of matter-wave jets from spinor BECs. (a) Zeeman shift of the $F = 1$ ground state manifold under a magnetic field B. The hyperfine interaction introduces a quadratic Zeeman shift $q > 0$ for ^{7}Li atoms. (b) A rf pulse flips atoms in the $|0\rangle$ state to the $(|\uparrow\rangle - |\downarrow\rangle)/\sqrt{2}$ state, which can be a highly excited spin state under a magnetic field ($q > |c|$). Quantum fluctuations produce two atom pairs of $|0\rangle$ state after spin-mixing collisions, and the excess internal energy is released in the kinetic energy of the atoms, flying in opposite directions because of momentum conservation. (c) Spin-resolved image of the matter-wave jets in $|0\rangle$ state with $q = 1.7$ kHz after a hold time of $t_h = 7.5$ ms. The image displays atoms in the horizontal plane, where we apply a field gradient during 16 ms of the time-of-flight (TOF). From left to right, the corresponding spins are $\{|\downarrow\rangle, |0\rangle, |\uparrow\rangle\}$. The inset represents the condensates remaining in the trap (dashed box). (d) Dressing the $|F = 1, m_F = -1\rangle$ state with $|F = 2, m_F = -2\rangle$ state by applying a microwave, we tune the q to have a negative value [39]. (e) After switching on the dressing field, the polar phase is no longer the ground state of the system, creating spin pairs ($|\uparrow\rangle$ and $|\downarrow\rangle$). Through the deexcitation process, the atom obtains kinetic energy from $|q|$. (f) After sufficient stimulated collisions, matter-wave jets of opposite spins are also observed.

Since the quadratic Zeeman energy far exceeds the condensate chemical potential, $\mu = h \times 350$ Hz, the matter-wave jets can escape the BECs and trapping potential.

As a complementary experiment, we also investigate the emission of matter-wave jets with $|\uparrow\rangle$ and $|\downarrow\rangle$ states from polar condensates. The polar phase becomes dynamically unstable when the quadratic Zeeman energy is negative [25], generating spin pairs of the $|\uparrow\rangle$ and $|\downarrow\rangle$ states [Fig. 1(e)]. Similar to the previous experiment, we observe two-dimensional matter-wave jets of the created spin states that have kinetic energy from the quadratic Zeeman energy, $E_k \simeq |q|$. One remarkable difference is that the matter-wave jets can naturally have a spin-momentum correlation (reminding the EPR state), which will be discussed after studying its generation mechanism.

The creation process can be well understood by investigating the early-time dynamics of matter-wave jets [Fig. 2(a)]. For both experiments listed above, initial dynamics are well described by a simple exponential function, $N_{\rm jet}(t) = N_{\rm jet}(0)e^{\gamma_e t}$, where the $\gamma_e \sim 160$ Hz. In the long-time limit, the jet populations saturate because of depletion of the source. The exponential growth dynamics

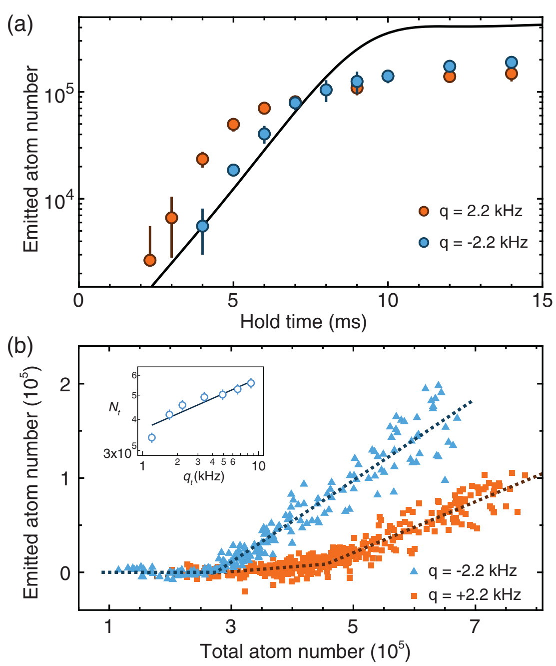

FIG. 2. (a) Dynamical generation of matter-wave jets. Emitted atom numbers over hold time for $q = \pm 2.2$ kHz. The error bars show 1 standard deviation. The solid line is obtained by numerical calculation based on the Bogoliubov theory of spinor condensate with the effective growth rate $\gamma_e = 160$ Hz [26]. (b) Threshold for jet formation. Emitted atom number after $t_h = 15$ ms under various initial atom numbers. To extract the threshold atom number N_t the data are fitted to bilinear curves (dashed lines). Inset: q_t dependence of N_t with power-law fit, $N_t \sim q_t^{0.2}$ (solid line). The error bars mean 95% confidence interval of the bilinear fits.

is a characteristic feature of the dynamical instability, in which spontaneously created atoms pairs are parametrically amplified [41,42]. The microscopic origin of such instability can be found in the existence of imaginary eigenfrequencies in the Bogoliubov quasiparticle (atom pair) spectrums [25]. The instability rate is maximized for particles with kinetic energy $E_k = |q| - c$, which is consistent with the observation within measurement uncertainty. The population growth rate of the quasiparticles is proportional to the spin-dependent interaction energy, $\gamma_b = 2|c|/h = 320$ Hz, which is 2 times higher than the observation. In order to ascribe the discrepancy, we consider a loss rate κ in a finite-sized system. When atoms with velocity v leave the condensates of radius R before sufficient spin-mixing collisions, it leads to an atom loss with a rate $\kappa \sim v/R$ [5,6]. In the experiments, we have $R = 100$ μm and $|q| = h \times 2.2$ kHz, and the escape rate (v/R) is evaluated to 100 Hz, which may account for the observed difference between γ_e and γ_b.

From this competing relation, we can expect that the burst mode only occurs when $\gamma_b > \kappa$. In other words, for runaway stimulated collisions, certain thresholds of atom number $(N > N_t)$ and quadratic Zeeman energy $(q < q_t)$ are required. For both initial conditions ($q/h = 2.2$ and $q/h = -2.2$ kHz), we observe a threshold behavior [Fig. 2(b)], and the threshold atom number increases with the external magnetic field [Fig. 2(b) inset]. An interesting observation is that, even with the same condensate density and magnitude of the quadratic Zeeman energy $|q|$, the emitted atom number for negative q is larger than that of positive q. Threshold behavior for positive q is smooth compared to its counterpart. Such differences can be attributed to the immiscible dynamics between the $|\uparrow\rangle$ and $|\downarrow\rangle$ states [43], which form magnetic spin domains after a hold time [Fig. 1(c) inset]. That is, the immiscible instability leads to population and phase mismatching between the two spin states, perturbing the collective matter-wave amplification process. The symmetry between positive and negative q might be reflected on a weak slope below the fitted N_t for positive q, starting from about 3.5×10^5. Such interplay between two strong instabilities (domain and jets formation) is worth investigating and we leave it for future research.

To uncover correlations in the matter-wave jets, we study the angular correlation functions,

$$C_{ij}(\phi) = \frac{\langle n_i(\phi')n_j(\phi' + \phi)\rangle}{\langle n_i(\phi')\rangle\langle n_j(\phi' + \phi)\rangle}, \qquad (1)$$

where $n_i(\phi)$ is the angular density of the emitted atoms in the $|i\rangle$ state and the brackets mean the angular and ensemble average, $\langle n_i\rangle = \langle(1/2\pi)\int n_i(\phi')d\phi'\rangle_{\rm ens}$. When the jets are in the $|0\rangle$ state for $q > |c|$, we study the correlation function $C_{00}(\phi)$, and when jets are in $|\uparrow\rangle$ and $|\downarrow\rangle$ states, we study spin versus momentum correlations by

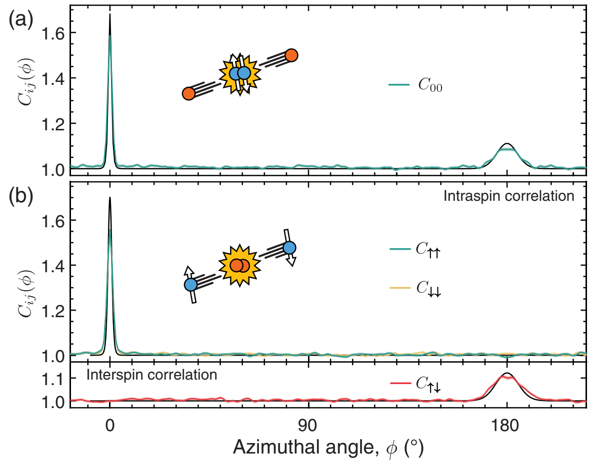

FIG. 3. Angular correlation functions of matter-wave jets after 28 ms of TOF under (a) $q = 2.7$ kHz and (b) $q = -2$ kHz. (b) The top shows the correlation between the same spins (intraspin) and the bottom shows the correlation between the opposite spins (interspin). Shaded areas mark one standard error based on 100–120 realizations. Black solid lines are time-dependent Bogoliubov calculations for the experimental parameters.

investigating the interspin $C_{\uparrow\downarrow}(\phi)$ and intraspin states $C_{\uparrow\uparrow}(\phi)$ and $C_{\downarrow\downarrow}(\phi)$ correlation functions. For both experiments, we observe one sharp peak near $\phi = 0°$ and the other broad peak near $\phi = 180°$. Both peaks are well displayed in C_{00} [Fig. 3(a)], and for matter-wave jets of opposite spin states, each peak can be found in the intra- and interspin state correlation functions [Fig. 3(b)], respectively.

The peak near $\phi = 0°$ is from the angular bunching [44] that represents the jet-shaped emission pattern. This is another consequence of the bosonic stimulation that contrasts to the incoherent scattering halo with a smooth angular profile [45]. In addition, it is also related to the statistics of the generated jets. The variance of $n_i(\phi)$ is $\mathrm{Var}[n_i(\phi)] = [C_{ii}(0) - 1]\langle n_i\rangle^2 + \langle n_i\rangle$. We see that $C_{ii}(0)$ is way above one and it is known to reach two for the ideal case [46]. When it reaches two, the statistics become completely thermal. As indicated in the study [47], the reduced density matrix of the quantum state displays a Bose-Einstein distribution because of the entropy associated with the correlated pairs. Indeed, the angular mode population for both spin states is well described by the thermal distribution [26]. A similar observation is also reported from Ref. [10], where the authors connect the emerging thermal distribution to the Unruh radiation, and the pair production Hamiltonian can be considered as a boosting transformation in an accelerating frame.

The other peak near $\phi = 180°$ implies momentum conservation of the emitted atom pair, and its width is broadened because of the near-field effect [7,46]. That is, the condensates cannot be regarded as a point source with the current expansion time so that different modes are overlapped in the detection area and interfere. According to the simple near-field model [7], about three modes ($N_m \simeq 3$) can be overlapped, reducing the correlation peaks to $C_{ij}(\phi = 180°) = 1 + 1/N_m^2 \simeq 1.1$. This is further supported by our time-dependent Bogoliubov calculation, which captures the angular correlation functions for all spin states at a quantitative level [Figs. 3(a) and 3(b)]. As we increase the expansion time in the calculation, these modes can be resolved, and the peak becomes higher and narrower.

Matter-wave jets of opposite spins are of particular interest, as the momentum correlation peak only appears for interspin state $C_{\uparrow\downarrow}(\phi = 180°)$, indicating strong correlation between spins and momentum, like EPR state. In a homogeneous system (or infinite expansion time limit), the quantum state after time evolution can be written as

$$\bigotimes_{\varepsilon_{\boldsymbol{k}} \approx |q|} \sum_{j=0}^{\infty} \lambda_j(t)[\hat{a}^\dagger_{\boldsymbol{k},\uparrow}\hat{a}^\dagger_{-\boldsymbol{k},\downarrow} + \hat{a}^\dagger_{\boldsymbol{k},\downarrow}\hat{a}^\dagger_{-\boldsymbol{k},\uparrow}]^j|\mathrm{vac}\rangle. \qquad (2)$$

The tensor product excludes opposite momentum ($\boldsymbol{k} = -\boldsymbol{k}$), and $\lambda_j(t) = \{[-i\tanh(ct)]^j/[j!\cosh^2(ct)]\}$ [26]. Here, the triplet Bell pair state $|\Psi_T\rangle = (\hat{a}_{k,\uparrow}\hat{a}_{-k,\downarrow} + \hat{a}_{k,\downarrow}\hat{a}_{-k,\uparrow})^\dagger|\mathrm{vac}\rangle$ constitutes the macroscopic entangled state, whose nonclassical correlation can be shown by interfering the two spin states. For example, under a spin rotation $(|\uparrow\rangle, |\downarrow\rangle \to [(|\uparrow\rangle \pm |\downarrow\rangle)/\sqrt{2}])$, the triplet state becomes another entangled state, $|\Psi_+\rangle = (\hat{a}_{k,\uparrow}\hat{a}_{-k,\uparrow} + \hat{a}_{k,\downarrow}\hat{a}_{-k,\downarrow})^\dagger|\mathrm{vac}\rangle$. Analyzing the angular correlation function $C_{ij}(\phi)$ for the entangled state $|\Psi_+\rangle$, the correlation peak near $\phi = 180°$ would appear only for the same spin state ($C_{\uparrow\uparrow}$ and $C_{\downarrow\downarrow}$). Increasing the spin rotation angle θ from 0 to 2π, these two quantum states are transformed into each other, displaying oscillations in the intra- and interspin state correlation peaks at $\phi = 180°$.

Taking the $|F = 2, m_F = 0\rangle$ upper hyperfine state as an intermediate state, the spin axis can be rotated by applying a microwave pulse [13]. When the matter-wave jets start to escape the trapped BECs ($t_h = 7.5$ ms), we apply the rotating pulse and measure the correlation functions. The momentum correlation peak in $C_{\uparrow\downarrow}(\phi = 180°)$ gradually disappears [Fig. 4(a)], while it simultaneously emerges in the intraspin correlation functions $C_{\uparrow\uparrow}$ and $C_{\downarrow\downarrow}$ [Fig. 4(b)]. Displaying the momentum-correlation peaks in Fig. 4(c) as a function of the rotation angle, we observe a clear oscillation with almost full contrast after 2π rotation. The observed oscillations are a clear signature that our spin state is in coherent superposition states with spin-momentum correlations. The next step would be the identification of the entanglement between counterpropagating matter waves with opposite spins. Adopting the separability criterion used in the bright squeezed vacuum state [48], we study the nonclassical correlations. Because of the near-field effect, a long expansion time (~150 ms) is

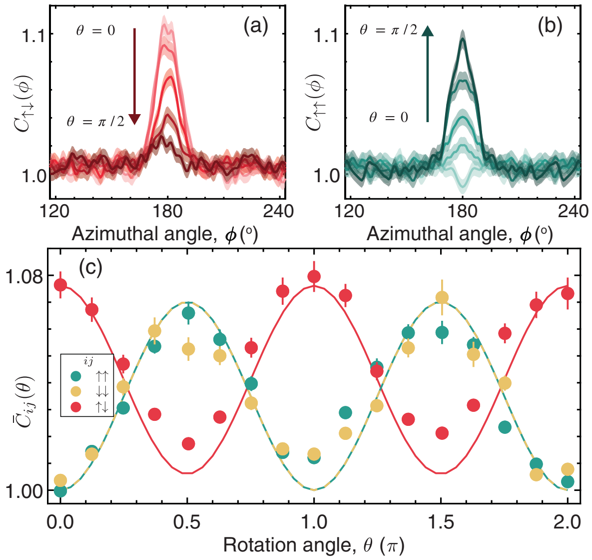

FIG. 4. As the spin rotation angle θ is increased from 0 to $\pi/2$, (a) the interspin correlation decreases (from light red to dark red), whereas (b) the intraspin correlation increases (from light green to dark green). The shades represent 1 standard deviation of the mean over 110 independent experiments. (c) Evolution of the averaged momentum correlation peak $\bar{C}_{ij}$ [mean value of $C_{ij}(\phi)$ in the interval $\phi \in [170°, 190°]$] under spin-axis rotation. Solid and dashed lines are numerical calculations accounting the field gradient effect [26]. The error bars represent 1 standard deviation of the mean.

required to probe the entanglement with current trap geometry, and we present the details in the Supplemental Material [26].

In conclusion, we have observed directional matter-wave jets of various spin states via the "superradiant" spin-mixing scattering process in using strongly ferromagnetic ^{7}Li spinor condensates. The matter-wave jets exhibit strong correlations between spins and momentum and hold the promise of being a macroscopic EPR state. This Letter opens up new perspectives for the study of quantum atom optics and quantum simulations using spinor BECs. It can be applied to precision measurement in an atom interferometer [20] to test Bell's inequality with massive particles [49] and to study nonequilibrium quantum dynamics with fast-moving impurities in a quantum liquid [50].

The authors thank Andrey Moskalenko and Young-Sik Ra for discussion. This work was supported by Samsung Science and Technology Foundation BA1702-06 and the National Research Foundation of Korea Grant No. 2019M3E4A1080401. S.C. acknowledges support from the Miller Institute for Basic Research in Science.

*jaeyoon.choi@kaist.ac.kr

[1] R. H. Dicke, Coherence in spontaneous radiation processes, Phys. Rev. 93, 99 (1954).
[2] S. Inouye, A. P. Chikkatur, D. M. Stamper-Kurn, J. Stenger, D. E. Pritchard, and W. Ketterle, Superradiant Rayleigh scattering from a Bose-Einstein condensate, Science 285, 571 (1999).
[3] P. Wang, L. Deng, E. W. Hagley, Z. Fu, S. Chai, and J. Zhang, Observation of Collective Atomic Recoil Motion in a Degenerate Fermion Gas, Phys. Rev. Lett. 106, 210401 (2011).
[4] M. G. Moore and P. Meystre, Theory of Superradiant Scattering of Laser Light from Bose-Einstein Condensates, Phys. Rev. Lett. 83, 5202 (1999).
[5] A. Vardi and M. G. Moore, Directional "Superradiant" Collisions: Bosonic Amplification of Atom Pairs Emitted from an Elongated Bose-Einstein Condensate, Phys. Rev. Lett. 89, 090403 (2002).
[6] L. W. Clark, A. Gaj, L. Feng, and C. Chin, Collective emission of matter-wave jets from driven Bose-Einstein condensates, Nature (London) 551, 356 (2017).
[7] H. Fu, L. Feng, B. M. Anderson, L. W. Clark, J. Hu, J. W. Andrade, C. Chin, and K. Levin, Density Waves and Jet Emission Asymmetry in Bose Fireworks, Phys. Rev. Lett. 121, 243001 (2018).
[8] A. P. Chikkatur, A. Görlitz, D. M. Stamper-Kurn, S. Inouye, S. Gupta, and W. Ketterle, Suppression and Enhancement of Impurity Scattering in a Bose-Einstein Condensate, Phys. Rev. Lett. 85, 483 (2000).
[9] L. Feng, J. Hu, L. W. Clark, and C. Chin, Correlations in high-harmonic generation of matter-wave jets revealed by pattern recognition, Science 363, 521 (2019).
[10] J. Hu, L. Feng, Z. Zhang, and C. Chin, Quantum simulation of Unruh radiation, Nat. Phys. 15, 785 (2019).
[11] L. Krinner, M. Stewart, A. Pazmiño, J. Kwon, and D. Schneble, Spontaneous emission of matter waves from a tunable open quantum system, Nature (London) 559, 589 (2018).
[12] C. Gross, H. Strobel, E. Nicklas, T. Zibold, N. Bar-Gill, G. Kurizki, and M. K. Oberthaler, Atomic homodyne detection of continuous-variable entangled twin-atom states, Nature (London) 480, 219 (2011).
[13] B. Lücke, M. Scherer, J. Kruse, L. Pezzé, F. Deuretzbacher, P. Hyllus, O. Topic, J. Peise, W. Ertmer, J. Arlt, L. Santos, A. Smerzi, and C. Klempt, Twin matter waves for interferometry beyond the classical limit, Science 334, 773 (2011).
[14] C. D. Hamley, C. S. Gerving, T. M. Hoang, E. M. Bookjans, and M. S. Chapman, Spin-nematic squeezed vacuum in a quantum gas, Nat. Phys. 8, 305 (2012).
[15] P. Kunkel, M. Prüfer, H. Strobel, D. Linnemann, A. Frölian, T. Gasenzer, M. Gärttner, and M. K. Oberthaler, Spatially distributed multipartite entanglement enables EPR steering of atomic clouds, Science 360, 413 (2018).
[16] K. Lange, J. Peise, B. Lücke, I. Kruse, G. Vitagliano, I. Apellaniz, M. Kleinmann, G. Tóth, and C. Klempt, Entanglement between two spatially separated atomic modes, Science 360, 416 (2018).
[17] W. Muessel, H. Strobel, D. Linnemann, D. B. Hume, and M. K. Oberthaler, Scalable Spin Squeezing for Quantum-Enhanced Magnetometry with Bose-Einstein Condensates, Phys. Rev. Lett. 113, 103004 (2014).
[18] I. Kruse, K. Lange, J. Peise, B. Lücke, L. Pezzè, J. Arlt, W. Ertmer, C. Lisdat, L. Santos, A. Smerzi, and C. Klempt,

Improvement of an Atomic Clock using Squeezed Vacuum, Phys. Rev. Lett. **117**, 143004 (2016).

[19] Y. Q. Zou, L. N. Wu, Q. Liu, X. Y. Luo, S. F. Guo, J. H. Cao, M. K. Tey, and L. You, Beating the classical precision limit with spin-1 Dicke states of more than 10,000 atoms, Proc. Natl. Acad. Sci. U.S.A. **115**, 6381 (2018).

[20] L. Pezzè, A. Smerzi, M. K. Oberthaler, R. Schmied, and P. Treutlein, Quantum metrology with nonclassical states of atomic ensembles, Rev. Mod. Phys. **90**, 035005 (2018).

[21] A. Einstein, B. Podolsky, and N. Rosen, Can quantum-mechanical description of physical reality be considered complete?, Phys. Rev. **47**, 777 (1935).

[22] H. Pu and P. Meystre, Creating Macroscopic Atomic Einstein-Podolsky-Rosen States from Bose-Einstein Condensates, Phys. Rev. Lett. **85**, 3987 (2000).

[23] L.-M. Duan, A. Sørensen, J. I. Cirac, and P. Zoller, Squeezing and Entanglement of Atomic Beams, Phys. Rev. Lett. **85**, 3991 (2000).

[24] S. J. Huh, K. Kim, K. Kwon, and J.-Y. Choi, Observation of a strongly ferromagnetic spinor Bose-Einstein condensate, Phys. Rev. Research **2**, 033471 (2020).

[25] Y. Kawaguchi and M. Ueda, Spinor Bose–Einstein condensates, Phys. Rep. **520**, 253 (2012).

[26] See Supplemental Material at http://link.aps.org/supplemental/10.1103/PhysRevLett.127.043401 for the description of (1) experimental details, (2) separability analysis, and (3) theoretical model, which includes Refs. [27–38].

[27] B. Lücke, J. Peise, G. Vitagliano, J. Arlt, L. Santos, G. Tóth, and C. Klempt, Detecting Multiparticle Entanglement of Dicke States, Phys. Rev. Lett. **112**, 155304 (2014).

[28] T. Mežnaršič, R. Žitko, T. Arh, K. Gosar, E. Zupanič, and P. Jeglič, Emission of correlated jets from a driven matter-wave soliton in a quasi-one-dimensional geometry, Phys. Rev. A **101**, 031601(R) (2020).

[29] C. Simon and D. Bouwmeester, Theory of an Entanglement Laser, Phys. Rev. Lett. **91**, 053601 (2003).

[30] J. Weiner, V. S. Bagnato, S. Zilio, and P. S. Julienne, Experiments and theory in cold and ultracold collisions, Rev. Mod. Phys. **71**, 1 (1999).

[31] J. M. Gerton, C. A. Sackett, B. J. Frew, and R. G. Hulet, Dipolar relaxation collisions in magnetically trapped ^{7}Li, Phys. Rev. A **59**, 1514 (1999).

[32] W. M. Itano, J. C. Bergquist, J. J. Bollinger, J. M. Gilligan, D. J. Heinzen, F. L. Moore, M. G. Raizen, and D. J. Wineland, Quantum projection noise: Population fluctuations in two-level systems, Phys. Rev. A **47**, 3554 (1993).

[33] J. Estève, C. Gross, W. A., G. S., and M. K. Oberthaler, Squeezing and entanglement in a Bose–Einstein condensate, Nature (London) **455**, 1216 (2008).

[34] M. F. Reidel, P. Böhi, Y. Li, T. W. Hänsch, A. Sinatra, and P. Treutlein, Atom-chip-based generation of entanglement for quantum metrology, Nature (London) **464**, 1170 (2010).

[35] W. Muessel, H. Strobel, M. Joos, E. Nicklas, I. Stroescu, J. Tomkovič, D. H. Hume, and M. K. Oberthaler, Optimized absorption imaging of mesoscopic atomic clouds, Appl. Phys. B **113**, 69 (2013).

[36] K. Hueck, N. Luick, L. Sobirey, J. Siegl, T. Lompe, H. Moritz, L. W. Clark, and C. Chin, Calibrating high intensity absorption imaging of ultracold atoms, Opt. Express **25**, 8670 (2017).

[37] M. V. Chekhova, G. Leuchs, and M. Zukowski, Bright squeezed vacuum: Entanglement of macroscopic light beams, Opt. Commun. **337**, 27 (2015).

[38] A. L. Fetter and J. D. Walecka, *Quantum Theory of Many-Particle Systems* (Dover Publications, New York, 2003).

[39] F. Gerbier, A. Widera, S. Fölling, O. Mandel, and I. Bloch, Resonant control of spin dynamics in ultracold quantum gases by microwave dressing, Phys. Rev. A **73**, 041602(R) (2006).

[40] J. M. Vogels, K. Xu, and W. Ketterle, Generation of Macroscopic Pair-Correlated Atomic Beams by Four-Wave Mixing in Bose-Einstein Condensates, Phys. Rev. Lett. **89**, 020401 (2002).

[41] C. Klempt, O. Topic, G. Gebreyesus, M. Scherer, T. Henninger, P. Hyllus, W. Ertmer, L. Santos, and J. J. Arlt, Parametric Amplification of Vacuum Fluctuations in a Spinor Condensate, Phys. Rev. Lett. **104**, 195303 (2010).

[42] The thermal population is less than 0.2 atoms per angular mode, indicating the observed amplification process is mostly caused by quantum fluctuations.

[43] S. De, D. L. Campbell, R. M. Price, A. Putra, B. M. Anderson, and I. B. Spielman, Quenched binary Bose-Einstein condensates: Spin-domain formation and coarsening, Phys. Rev. A **89**, 033631 (2014).

[44] R. H. Brown and R. Q. Twiss, Correlation between photons in two coherent beams of light, Nature (London) **177**, 27 (1956).

[45] A. Perrin, H. Chang, V. Krachmalnicoff, M. Schellekens, D. Boiron, A. Aspect, and C. I. Westbrook, Observation of Atom Pairs in Spontaneous Four-Wave Mixing of Two Colliding Bose-Einstein Condensates, Phys. Rev. Lett. **99**, 150405 (2007).

[46] Z. Wu and H. Zhai, Dynamics and density correlations in matter-wave jet emission of a driven condensate, Phys. Rev. A **99**, 063624 (2019).

[47] G. I. Mias, N. R. Cooper, and S. M. Girvin, Quantum noise, scaling, and domain formation in a spinor Bose-Einstein condensate, Phys. Rev. A **77**, 023616 (2008).

[48] T. S. Iskhakov, I. N. Agafonov, M. V. Chekhova, and G. Leuchs, Polarization-Entangled Light Pulses of 10^5 Photons, Phys. Rev. Lett. **109**, 150502 (2012).

[49] J. S. Bell, On the Einstein Podolsky Rosen paradox, Phys. Phys. Fiz. **1**, 195 (1964).

[50] C. J. M. Mathy, M. B. Zvonarev, and E. Demler, Quantum flutter of supersonic particles in one-dimensional quantum liquids, Nat. Phys. **8**, 881 (2012).